Original Research

Effects of the Anterolateral Ligament and Anterior Cruciate Ligament on Knee Joint Mechanics

A Biomechanical Study Using Computational Modeling

Kyoung-Tak Kang,* MD, PhD, Yong-Gon Koh,† MD, Kyoung-Mi Park,* MD, Chong-Hyuk Choi,‡ MD, PhD, Min Jung,‡ MD, PhD, Hyunik Cho,‡ MD, and Sung-Hwan Kim,‡§ MD, PhD

Investigation performed at Yonsei University College of Medicine, Severance Hospital, Seoul, Republic of Korea

Background: Recent studies on lateral knee anatomy have reported the presence of a true ligament structure, the anterolateral ligament (ALL), in the anterolateral region of the knee joint. However, its biomechanical effects have not been fully elucidated.

Purpose: To investigate, by using computer simulation, the association between the ALL and anterior cruciate ligament (ACL) under dynamic loading conditions.

Study Design: Descriptive laboratory study; Level of evidence, 5.

Methods: The authors combined medical imaging from 5 healthy participants with motion capture to create participant-specific knee models that simulated the entire 12 degrees of freedom of tibiofemoral (TF) and patellofemoral (PF) joint behaviors. These dynamic computational models were validated using electromyographic data, muscle activation data, and data from previous experimental studies. Forces exerted on the ALL with ACL deficiency and on the ACL with ALL deficiency, as well as TF and PF contact forces with deficiencies of the ACL, ALL, and the entire ligament structure, were evaluated under gait and squat loading. A single gait cycle and squat cycle were divided into 11 time points (periods 0.0-1.0). Simulated ligament forces and contact forces were compared using nonparametric repeated-measures Friedman tests.

Results: Force exerted on the ALL significantly increased with ACL deficiency under both gait- and squat-loading conditions. With ACL deficiency, the mean force on the ALL increased by 129.7% under gait loading in the 0.4 period ($P < .05$) and increased by 189% under high flexion during the entire cycle of squat loading ($P < .05$). A similar trend of significantly increased force on the ACL was observed with ALL deficiency. Contact forces on the TF and PF joints with deficiencies of the ACL, ALL, and entire ligament structure showed a complicated pattern. However, contact force exerted on TF and PF joints with respect to deficiencies of ACL and ALL significantly increased under both gait- and squat-loading conditions.

Conclusion: The results of this computer simulation study indicate that the ACL and the ALL of the lateral knee joint act as secondary stabilizers to each other under dynamic load conditions.

Keywords: anterior cruciate ligament; anterolateral ligament; computational analysis; knee injury

Data on the anatomy, kinematics, injury mechanisms, and treatment of the anterolateral aspect of the knee joint are limited.[32] The interaction between the dynamic and static stabilizers of the knee joint is complicated.[9] In particular, the lateral side of the knee joint relies on these stabilizers because of its inherent bony instability from the opposite convex surfaces.[41] No standard anatomical terminology for the soft tissue structures near the anterolateral aspect of the knee joint is used in orthopaedic clinical practice.[6] Functional studies using anatomical specimens may overcome this lack of knowledge and provide acceptable standard anatomical, clinical, and operative nomenclature.[13] Recent anatomical studies have described the points of origin and the anterolateral ligament (ALL) insertion of the knee joint.[11,40] Despite the lack of specific biomechanical tests for the role of the ALL in generating anterolateral rotatory knee instability, a previous

The Orthopaedic Journal of Sports Medicine, 10(4), 23259671221084970
DOI: 10.1177/23259671221084970

study demonstrated the importance of pivot-shift test scores in anterolateral capsule injury.[26] The importance of this structure in anterior cruciate ligament (ACL) injuries is not a novel discovery.[12,35,38] There has been renewed interest in recent years in the anterolateral structures of the knee joint, and our understanding of the association of these structures to ACL injury and the resulting rotational instability has evolved. The natural evolution of an ACL rupture with recurrent instability is progressive degeneration on the medial meniscus and the articular cartilage, which is observed in 60% to 90% of patients, respectively, about 10 to 20 years after the initial injury.[27,29,31] Zens et al[42] analyzed changes in ALL length during passive knee motion. Kennedy et al[17] characterized the anatomical and radiographic locations and structural properties of the ALL and provided quantitative data. Rasmussen et al[34] found that combined sectioning of the ALL and ACL would lead to increased internal rotation and axial plane translation during a pivot-shift test when compared with isolated sectioning of the ACL. Nitri et al[28] investigated the biomechanical function of an anatomical ALL reconstruction in the setting of a combined ACL and ALL injury. Results from these 4 studies suggest that the ALL is an important lateral knee structure that provides rotatory stability to the knee joint. However, to the best of our knowledge, the association between the ALL and ACL under dynamic loading conditions has not been investigated in vitro.

Our objective in this study was therefore to develop and validate a participant-specific musculoskeletal (MSK) lower extremity model that allows for 12-degrees-of-freedom (DOF) motion at both the tibiofemoral (TF) and patellofemoral (PF) joints by combining medical imaging data with motion capture data for 5 healthy participants (4 male and 1 female) to create participant-specific knee models. We hypothesized that insufficiency of the ACL or ALL would cause an abnormal increase not only to the ligament force of each other but also to the joint force under dynamic joint-loading conditions.

METHODS

Experimental Procedures

After receiving approval from the hospital's institutional review board and written informed consent from the 5 participants, participant-specific data were used to develop the participant-specific MSK model, and electromyography (EMG) signals were used during motion capture. Four male participants and 1 female participant who had no medical history of lower extremity problems participated in this study. The mean age, height, and weight of the participants were 33.0 ± 4.4 years (range, 26-36 years), 175 ± 7.4 cm (range, 163-182 cm), and 75.6 ± 6.7 kg (range, 65-83 kg), respectively. The participants performed gait and squatting activities, and ground-reaction forces were measured using a force plate (Figure 1). Tracks of marker locations were measured using a 3-dimensional (3D) motion capture system (Vicon). EMG signals were recorded from the following muscles using an EMG sensor (Delsys): gluteus maximus, rectus femoris, vastus lateralis, biceps femoris, semimembranosus, gastrocnemius medialis, tibialis anterior, and soleus medialis. Raw data from the EMG signals were transformed into muscle activation data by root-mean-square analysis.

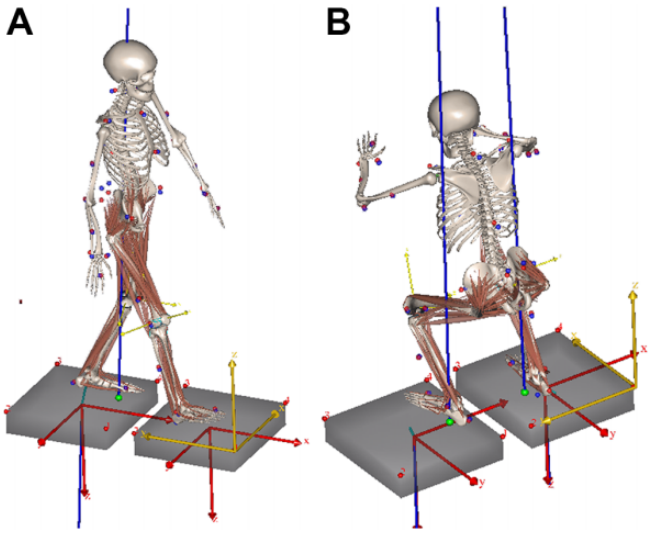

Figure 1. Participant-specific musculoskeletal models during (A) gait and (B) squat conditions.

To evaluate the predicted muscle activation, an EMG-to-activation model was developed to represent the underlying muscle activation dynamics. Muscle-tendon lengths and moments of muscles crossing the knee joint were determined from joint kinematics using the 3D anatomic model. Muscle activation was determined using a second-order discrete nonlinear model with rectified and low-pass filtered EMG as input. The process of transforming EMG data to muscle activation data has been described previously.[24]

Computational Model

The 5 participant-specific models were developed using AnyBody Version 6.0.5 (AnyBody Technology), which is a commercial software package for MSK simulation. The generic lower

§Address correspondence to Sung-Hwan Kim, MD, PhD, Department of Orthopedic Surgery, Arthroscopy and Joint Research Institute, Yonsei University College of Medicine, Gangnam Severance Hospital, 211 Eonju-ro, Gangnam-gu, Seoul, 06273, Republic of Korea (email: orthohwan@gmail.com).
*Department of Mechanical Engineering, Yonsei University, Seoul, Republic of Korea.
†Joint Reconstruction Center, Department of Orthopaedic Surgery, Yonsei Sarang Hospital, Seoul, Republic of Korea.
‡Department of Orthopedic Surgery, Arthroscopy and Joint Research Institute, Yonsei University College of Medicine, Seoul, Republic of Korea.
Final revision submitted October 14, 2021; accepted December 22, 2021.
The authors declared that they have no conflicts of interest in the authorship and publication of this contribution. AOSSM checks author disclosures against the Open Payments Database (OPD). AOSSM has not conducted an independent investigation on the OPD and disclaims any liability or responsibility relating thereto.
Ethical approval for this study was obtained from Yonsei University, Gangnam Severance Hospital (reference No. 3-2016-0271).

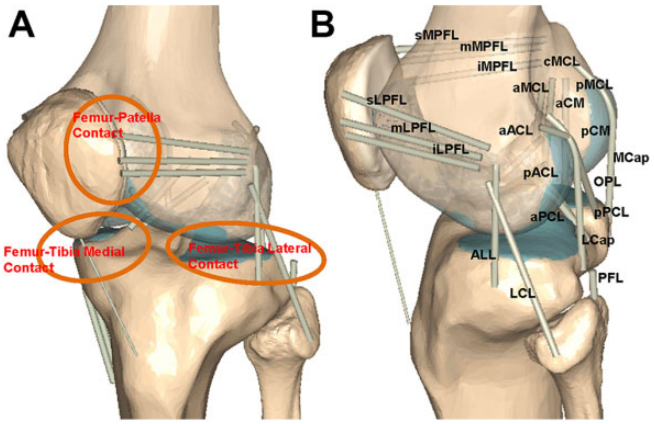

Figure 2. Participant-specific musculoskeletal models with (A) contact conditions and (B) 21 ligament bundles: anteromedial (aACL) and posterolateral (pACL) bundles of the anterior cruciate ligament; anterolateral (aPCL) and posteromedial (pPCL) bundles of the posterior cruciate ligament; anterolateral structures; lateral collateral ligament (LCL); popliteofibular ligament (PFL); medial collateral ligament (anterior portion [aMCL], central portion [cMCL], and posterior portion [pMCL]); deep medial collateral ligament (anterior portion [aCM] and posterior portion [pCM]); medial (MCap) and lateral (LCap) posterior capsules; oblique popliteal ligament; medial patellofemoral ligament (superior [sMPFL], middle [mMPFL], and inferior [iMPFL]); and lateral patellofemoral ligament (superior [sLPFL], middle [mLPFL], and inferior [iLPFL]). Anterolateral ligament (ALL); oblique popliteal ligament (OPL).

extremity MSK model is based on the Twente Lower Extremity Model anthropometric database.[20] The MSK model is actuated by approximately 160 muscle units. It has been previously validated for predicting muscle and joint reaction forces in human lower limbs during locomotion.[1,7]

Three-dimensional bone and soft tissue models were reconstructed from computed tomography (CT) and magnetic resonance imaging (MRI) scans in our previous study.[14,19,21] Ligament insertion points were also observed in the MRI sets, and descriptions can be found in the literature.[14,19,21] Two experienced orthopaedic surgeons (including S.-H.K.) determined the locations of the ligaments independently.[16]

By using 3D femoral and tibial models of the 5 participants, the femur and tibia in AnyBody were scaled with nonlinear radial basis functions as scaling laws. The remaining parts were scaled using an optimization scheme that minimizes the difference between the model markers and recorded marker positions. The knee joint in this study was considered to have 12 DOF (TF, 6 DOF; PF, 6 DOF).[15] The hip and ankle joints were considered to have 2 and 3 DOF, respectively.[15] For the hip joint, those are flexion/extension, abduction/adduction. For the ankle joint, those are abduction/adduction, dorsiflexion/plantarflexion, and eversion/inversion.

The attachment points in the AnyBody model were modified using participant-specific attachment sites. As shown in Figure 2, a total of 21 ligament bundles were modeled: the ACL (anteromedial bundle of the ACL [aACL]; posterolateral bundle of the ACL [pACL]); posterior cruciate ligament (PCL), which included the anterolateral and posteromedial bundles of the PCL; ALL; lateral collateral ligament (LCL); popliteofibular ligament; medial collateral ligament, which included the anterior, central, and posterior portions; deep medial collateral ligament, which included the anterior and posterior portions; medial and lateral posterior capsules; oblique popliteal ligament; medial PF ligament (superior, middle, and inferior); and lateral PF ligament (superior, middle, and inferior).

The stiffness-force relationship of the ligaments in this model were defined as follows to produce nonlinear elastic characteristics in slack regions[3]:

$$f(\epsilon) = \begin{cases} \dfrac{k\epsilon^2}{4\epsilon_1}, & 0 \le \epsilon \le \epsilon_1 \\ k(\epsilon - \epsilon_1), & \epsilon > 2\epsilon_1 \\ 0, & \epsilon < 0 \end{cases}$$

$$\epsilon = \frac{l - l_0}{l_0}$$

$$l_0 = \frac{l_r}{\epsilon_r + 1}$$

where $f(\epsilon)$ is the current force, k is the stiffness, ϵ is the strain, and ϵ_1 was assumed to be constant at 0.03. The ligament bundle slack length, l_0, can be calculated from the reference bundle length, l_r, and the reference strain, ϵ_r, in the upright reference position.

Most of the stiffness and reference strain values were adopted from the literature, with some modification.[3,25,37] Menisci were modeled as linear springs to simulate their equivalent resistance.[23] A wrapping surface comprising a cylinder and an ellipsoid was applied to prevent penetration of bone by the ligament. One to 3 wrapping surfaces were applied to each ligament to wrap the geometry of the bone.

Figure 2 shows 3 rigid-rigid standard tessellation language–based contacts defined in the TF and PF joints. Three deformable contact models were defined between the femoral and tibial components, and between the femoral component and patellar button. These contact forces were proportional to the penetration volume and so-called pressure module.[25] To calculate the value of the pressure module, an equation derived by Fregly et al[8] was used.

Inverse Dynamic Simulation and Loading Conditions

Before running the inverse dynamic analysis, the kinematics of each trial were calculated on the basis of motion capture data. Kinematic optimization was used for this purpose. To optimize kinematic model parameters, ground-reaction forces and motion capture marker trajectory data were imported into AnyBody. The optimization objective was to minimize the difference between the AnyBody model marker trajectories and the motion capture

marker trajectories. After kinematic optimization, inverse dynamic analysis was performed. The muscle recruitment criterion used in this study was cubic polynomial. Muscle activation and ligament forces were calculated through inverse dynamic analysis, and muscle activations were compared with EMG signals. Internal rotation torque tests for rotational laxity under intact and both ACL and ALL conditions with 5 N·m of torque at 0°, 30°, 60°, and 90° of flexion were compared with previous experimental studies.[34,36]

To define the influence of resection of ALL and ACL structures on the ACL and ALL, respectively, the forces on the ALL and ACL with deficiencies of the individual components were investigated under gait and squat loading conditions. In addition, contact forces on the TF and PF joints were evaluated with deficiencies of the ACL, ALL, and entire ligament structure under gait and squat loading conditions.

Statistical Analysis

A single gait cycle and squat cycle were divided into 11 time points (periods 0.0-1.0). Calculated ligament forces and contact forces in each simulated model were compared with the corresponding simulation data from the same knee at the same phase of the cycle. Simulated ligament forces and contact forces for deficiency of the ACL, ALL, and both ACL and ALL were compared using nonparametric repeated-measures Friedman tests. Post hoc comparisons were performed between each ligament-deficient status and the intact knee condition using the Wilcoxon signed-rank test with Holm correction. Statistical analyses were performed using SPSS for Windows (Version 20.0.0; IBM Corp). Statistical significance was set at $P < .05$ for all comparisons.

RESULTS

Comparison Between Experimental EMG and Muscle Activation Measurements from Computational Simulation and Previous Experimental Studies

The greatest muscle activities predicted from the 4 computational models were consistent with the transformed EMG measurements under the gait and squat loading conditions (Supplemental Figures S1 and S2). For the intact and deficient ACL and ALL models, the mean values for the internal rotation from computational simulation were within the range of values from previous experimental studies[34,36] (Figure 3).

Forces Exerted on the ACL With ALL Deficiency and the ALL With ACL Deficiency

The force exerted on the aACL and pACL with ALL deficiency and the force exerted on the ALL with ACL deficiency under gait and squat loading conditions are shown in Figure 4. Forces exerted on the aACL and pACL during the gait-loading condition significantly increased in the stance phase as the ALL became deficient. The mean forces on the aACL and pACL increased significantly by

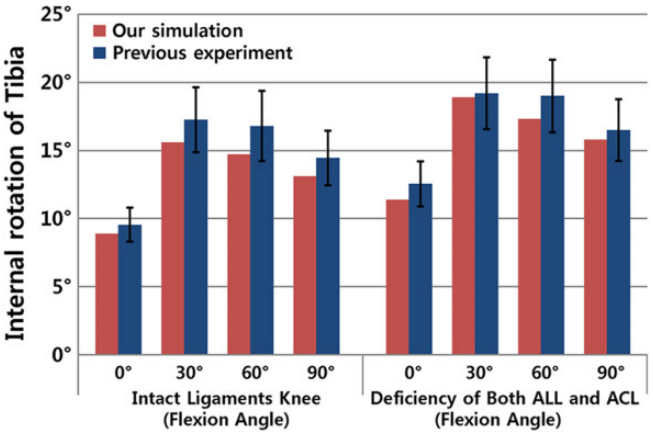

Figure 3. Comparison between the current study and previous studies[34,36] of the internal tibial rotation in the internal rotation torque between intact and anterolateral ligament (ALL)– and anterior cruciate ligament (ACL)–deficient conditions at 0°, 30°, 60°, and 90° of flexion. Error bars represent SDs.

42.5% ($P < .05$) and 62.5% ($P < .05$), respectively, in the 0.2 and 0.3 periods with ALL deficiency during the stance phase's gait-loading condition. The mean force on the ALL significantly increased by 129.7% ($P < .05$) in the 0.4 period with ACL deficiency during the stance phase's gait-loading condition.

The mean force on the aACL from the 0.6 to 1.0 period and the pACL from the 0.8 to 1.0 period significantly increased by 20.2% ($P < .05$) and 89.4% ($P < .05$), respectively, with ALL deficiency during the squat-loading condition. The mean force on the ALL significantly increased the entire period by 189% ($P < .05$) under high flexion with ACL deficiency during squat loading (Figure 4).

Contact Force With Deficiencies of the ACL, ALL, and Entire Ligament Structures of the Knee Joint Under Gait- and Squat-Loading Conditions

Figure 5 shows the contact forces on the TF and PF with deficiencies of the ACL, ALL, and entire ligament structure during gait loading. The mean contact forces on the TF and PF joints were 1.7 ± 0.47 ($P < .01$) and 1.3 ± 0.23 ($P < .01$) times greater than body weight (BW) at 1360 ± 303.9 N and 1060 ± 203.5 N, respectively, for an intact model.

The mean contact force on the medial side was greater than that on the lateral side for an intact model during gait loading. The mean contact forces on the medial TF joint significantly increased with deficiency of ACL during the 0.0 and 1.0 periods and with deficiency of both ACL and ALL during the entire period under the gait cycle's loading condition. The deficient ACL significantly increased lateral contact force in the TF joint during the initial stance phase under the gait cycle's loading condition. The deficiency of ACL and ALL significantly increased lateral contact force in the TF joint during the stance and swing phase under the gait cycle's loading

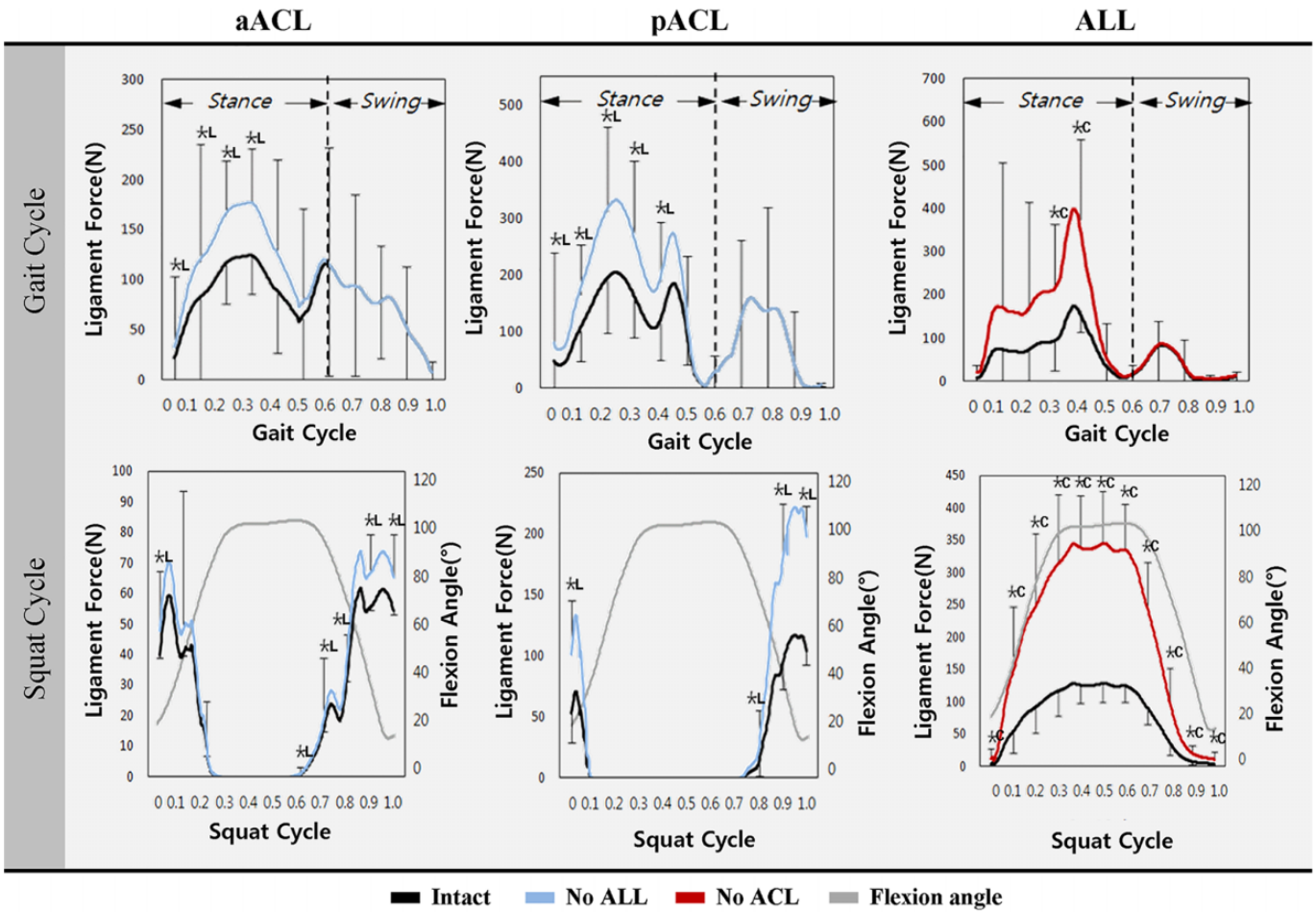

Figure 4. Mean force exerted on the anterior cruciate ligament (ACL) and anterolateral ligament (ALL) with deficiencies of the ALL and ACL during gait- and squat-loading conditions. Error bars indicate SDs. Significant differences ($P < .05$) were found between the intact and ALL-deficient condition (*L) and between the intact and ACL-deficient condition (*C). aACL, anteromedial bundle of the ACL; pACL, posterolateral bundle of the ACL.

condition. However, the deficiency of ALL did not significantly increase the medial contact forces in the TF and PF joints under the gait cycle's loading condition.

The mean contact forces on the TF and PF joints with deficiencies of the ACL, ALL, and entire ligament structure under the squat loading condition are shown in Figure 6. The mean contact forces on the TF and PF joints were 1.95 ± 0.89 ($P < .01$) and 3.78 ± 0.36 ($P < .01$) times greater than BW at 1490 ± 613.2 N and 2890 ± 288.6 N, respectively, with an intact model.

The mean contact forces on the medial TF joint increased in low flexion and decreased in high flexion with ACL deficiency under the squat-loading condition. The mean contact forces on the medial TF joint significantly increased with deficiency of ACL during the 0.1 to 0.2 period and with deficiency of both ACL and ALL during the 0.2 to 0.6 period under the squat-loading condition. The deficient ACL significantly increased the lateral contact force in the TF joint during low flexion angle under the squat-loading condition. The deficiency of ACL and ALL significantly increased the lateral contact force in the TF joint during the 0.5 to 1.0 period under the squat-loading condition. However, the deficiency of ALL did not significantly increase the medial and lateral contact forces in the TF joint under the squat-loading condition. ACL deficiency had no significant effect on the mean contact force on the PF joint during squat loading. However, the mean contact force on the PF joint increased by 24% and 28% with deficiencies of the ALL and entire ligament structure, respectively, under the squat-loading condition. The deficiency of ALL in the 0.3 to 0.5 period and both ACL and ALL in high flexion significantly increased the contact force in the PF joint under the squat-loading condition.

DISCUSSION

Our study demonstrated the hypothesis that the ACL and the ALL of the lateral knee joint assist as secondary stabilizers of each other under dynamic load conditions. The

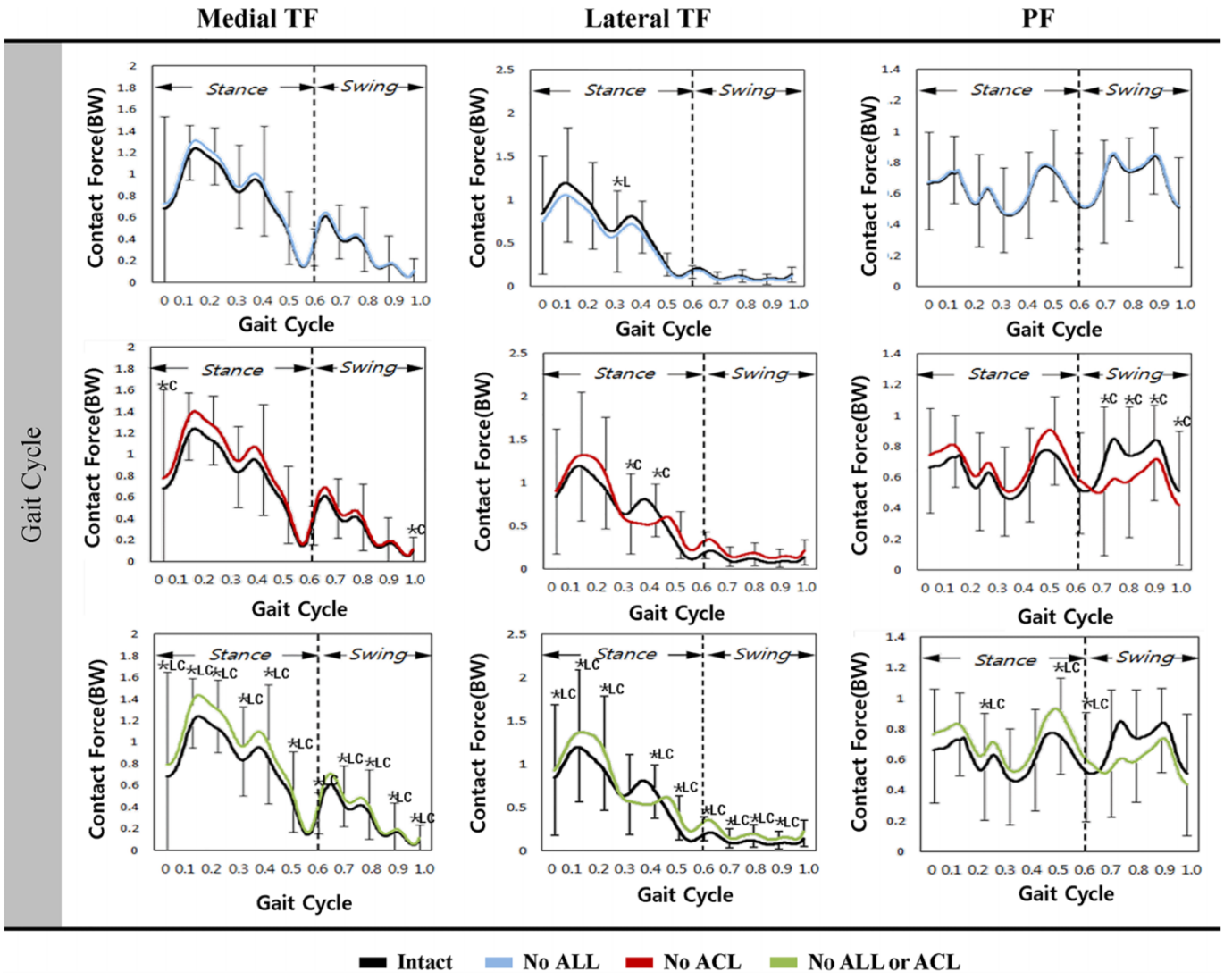

Figure 5. Mean contact forces on the tibiofemoral (TF) and patellofemoral (PF) joints with deficiencies of the anterolateral ligament (ALL), anterior cruciate ligament (ACL), and entire ligament structure under the gait-loading condition. Error bars indicate SDs. There were significant differences ($P < .05$) between the intact and ALL-deficient condition (*L), between the intact and ACL-deficient condition (*C), and between the intact and both ALL- and ACL-deficient conditions (*LC). BW, body weight.

mean force on the ALL increased by 129.7% ($P < .05$) in the 0.4 period with ACL deficiency under the gait-loading condition and in the entire period by 189% ($P < .05$) under high flexion with ACL deficiency during squat loading. Deficiency of the ACL and ALL increased the forces on the ALL and ACL, respectively, while deficiency of both the ACL and ALL increased the contact forces on the TF and PF joints.

Lateral instability is less commonly reported but is more severe than medial instability of the knee joint.[2] Recently, there has been an increase in the number of biomechanical and anatomical studies of the anterolateral capsule structures.[17,28,31,34,42] Only a few biomechanical studies have investigated the function of the structure. However, some authors have reported the results of surgical treatment of ACL injuries.[9] The results of kinematic analyses, cadaveric experiments, and evaluation of force exerted on ligaments and ligament-length pattern changes on CT under quasi-static conditions have been reported.[17,24,28,30,34,42] It should be noted that cadavers used in in vitro experiments are usually donated from the aged population; therefore, loosening in the experimental setting as well as some attenuation of the tissue itself because of the repetitive loading to the specimen could occur.[5] No study, to the best of our knowledge, has evaluated the ligament or contact forces on the TF and PF joints with deficiencies of the ACL, ALL, and entire ligament structure under loading conditions during daily activities.

We developed a dynamic model in this study to evaluate the forces exerted on the ACL and ALL, the contact forces on the TF and PF joints, and muscle activation with deficiencies of the ACL, ALL, and entire ligament structure in the knee joint under gait- and squat-loading conditions

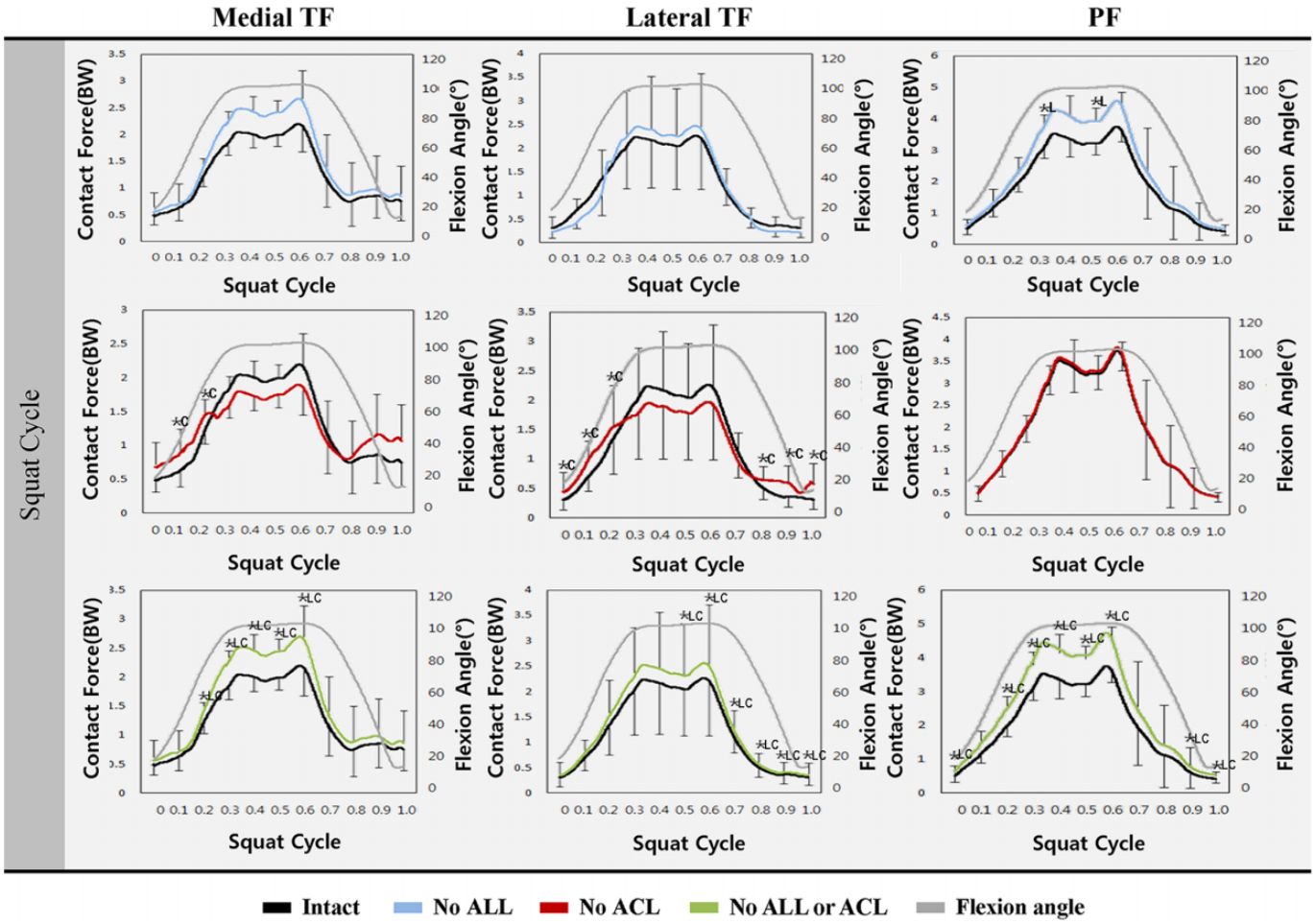

Figure 6. Mean contact forces on the tibiofemoral (TF) and patellofemoral (PF) joints with deficiencies of the anterolateral ligament (ALL), anterior cruciate ligament (ACL), and entire ligament structure under the squat-loading condition. Error bars indicate SDs. Significant differences ($P < .05$) between the intact and ALL-deficient condition (*L), between the intact and ACL-deficient condition (*C), and between the intact and both ALL- and ACL-deficient condition (*LC) were found. BW, body weight.

using the MSK model. Errors can occur in the prediction of muscle activities when using a computation model because of the muscle redundancy problem under inverse dynamic conditions and inaccuracy in muscle moment arms. There may have been significant differences in muscle activations because some muscles were sectioned into multiple branches in the AnyBody MSK model, and the EMG signal was more related to the activity of the large muscle group closest to the electrode.

We found a strong interaction between the ACL and ALL under loading conditions during daily activities. Increases in the ACL force according to ALL deficiency were similar between the gait- and squat-loading conditions. The mean force on the ALL increased by 129.7% ($P < .05$) in the 0.4 period with ACL deficiency under the gait-loading condition and in the entire period by 189% ($P < .05$) under high flexion with ACL deficiency during squat loading. However, the increase in force exerted on the ALL was more sensitive to squat loading than gait loading. In other words, the force exerted on the ALL was influenced more during high flexion than low flexion. Parsons et al[30] reported that the ALL does not affect resistance to the anterior tibial drawer during knee flexion and that the LCL is not a primary stabilizer in either the anterior drawer or internal rotation. However, they found that the ALL is a primary stabilizer of internal rotation of the tibia in high flexion. Despite the differences in participants and loading conditions between the robotic testing systems and computational model, both suggest that the ALL plays an important role in high flexion.

ACL deficiency causes degeneration of the articular cartilage in the TF joint, which could aggravate progressive osteoarthritis.[27,29,31] Based on previous in vivo lower extremity measurements, our results support the finding that a load up to 3 times greater than BW is exerted along the hip, TF, and PF joints during daily activities.[10] The contact forces exerted on the TF and PF in this study showed good agreement with the results from previous studies.[33,37,39] The medial contact forces were greater than the lateral contact forces under both gait- and squat-

loading conditions. In addition, the ratio of BW to contact forces was consistent with those reported in previous studies.[33,37,39] In this study, the contact force on the PF joint increased compared with that on the TF joint in high flexion, similar to the results of a previous study.[39] The contact forces on the medial side of the TF joint all increased with deficiencies of the ALL, ACL, and entire ligament structure in the gait-loading condition. However, the ACL and ALL deficiencies had no synergistic effect on the contact force on the medial TF joint. The contact force on the lateral TF joint had a complicated pattern. Especially for the ACL, the contact force on the lateral TF joint locally increased and decreased in the stance phase but increased in the swing phase during gait loading. However, contact force on the lateral TF joint decreased with ALL deficiency during gait loading. The contact forces on the PF joint increased in the swing phase and decreased in the stance phase with ACL deficiency during gait loading.

Interestingly, contact force on the medial TF joint increased with deficiencies of the ACL, ALL, and entire ligament structure. However, for ACL deficiency, it increased in low flexion and decreased in high flexion. This trend was also found in the contact force on the lateral TF joint with ALL deficiency. In this case, it decreased in low flexion and increased in high flexion. ACL deficiency decreased the contact force in the lateral TF joint, and a similar trend was found in the PF joint during squat loading. ACL deficiency did not influence the contact force on the PF joint, but deficiencies of the ALL and entire ligament structure increased the contact force on the PF joint in high flexion. In addition, there are 2 things that can prompt a change to deficient ligaments: 3D knee kinematics and the force of each ligament. If a primary ligament is torn, then it is thought that other ligaments will receive increased forces because of their role as secondary stabilizers. Our model helps to predict the forces acting on the ACL and ALL. However, the ALL remains controversial, as it not easily identified on MRI; thus, studies with additional insertion points for the ALL may be needed.

Limitations

Several limitations should be mentioned regarding this study. First, the insertion point of the ALL was manually modified to match the geometry of the patient's knee anatomy in the model.[6,12,17] The result could vary depending on the position of the ALL. However, there is a large deviation in the position of the ALL, and the ALL is a structure that cannot be easily determined by using MRI alone. Second, sample size was small because it is time-consuming and computationally expensive to develop participant-specific models. In many previous studies, only a single participant-specific model had been used to assess the surgical technique or injury mechanism.[1,4,9,15,19,21,25,37,39] In addition, it is also noted that the proportion of men in biomechanical study data is 80%, and thus there is a limit to female models. Third, deficient-ligament models were validated by using data from the literature rather than obtaining our own measurements. However, this approach is widely used in orthopaedic biomechanics research.[15,18,22] The advantage of computational simulation of a participant was that we could determine the effects of deficiency of the ACL or ALL on the validated participant-specific models and exclude effects of variables such as weight, height, bony geometry, and ligament properties. Fourth, the material properties of the ligaments in the model were based on literature reports. Fifth, the limitation of DOF at the hip and ankle can cause significant measurement variances by not accounting for motion outside of those DOF. Finally, ground-reaction forces were measured directly from the feet during gait and squat simulations. Future improvements could be achieved by applying a ground-contact model that allows reaction force simulation and incorporates foot-floor interactions.[22]

CONCLUSION

The results of this study indicate that the ALL is an important lateral knee structure in daily dynamic activity. The ACL and the ALL of the lateral knee joint assist as secondary stabilizers of each other under dynamic load conditions.

Supplemental material for this article is available at http://journals.sagepub.com/doi/suppl/10.1177/23259671221084970.

REFERENCES

1. Ali N, Andersen MS, Rasmussen J, Robertson DG, Rouhi G. The application of musculoskeletal modeling to investigate gender bias in non-contact ACL injury rate during single-leg landings. *Comput Methods Biomech Biomed Eng*. 2014;17(14):1602-1616.
2. Bertoia JT, Urovitz EP, Richards RR, Gross AE. Anterior cruciate reconstruction using the MacIntosh lateral-substitution over-the-top repair. *J Bone Joint Surg Am*. 1985;67(8):1183-1188.
3. Blankevoort L, Huiskes R. Ligament-bone interaction in a three-dimensional model of the knee. *J Biomech Eng*. 1991;113(3):263-269.
4. Chen Z, Zhang X, Ardestani MM, et al. Prediction of in vivo joint mechanics of an artificial knee implant using rigid multi-body dynamics with elastic contacts. *Proc Inst Mech Eng H*. 2014;228(6):564-575.
5. Chun YM, Kim SJ, Kim HS. Evaluation of the mechanical properties of posterolateral structures and supporting posterolateral instability of the knee. *J Orthop Res*. 2008;26(10):1371-1376.
6. Dodds AL, Halewood C, Gupte CM, Williams A, Amis AA. The anterolateral ligament: anatomy, length changes and association with the Segond fracture. *Bone Joint J*. 2014;96(3):325-331.
7. Forster E. *Predicting Muscle Forces in the Human Lower Limb During Locomotion*. VDI Verlag; 2004.
8. Fregly BJ, Bei Y, Sylvester ME. Experimental evaluation of an elastic foundation model to predict contact pressures in knee replacements. *J Biomech*. 2003;36(11):1659-1668.
9. Guenther D, Griffith C, Lesniak B, et al. Anterolateral rotatory instability of the knee. *Knee Surg Sports Traumatol Arthrosc*. 2015;23(10):2909-2917.

10. Heinlein B, Kutzner I, Graichen F, et al. ESB Clinical Biomechanics Award 2008: complete data of total knee replacement loading for level walking and stair climbing measured in vivo with a follow-up of 6-10 months. *Clin Biomech (Bristol, Avon)*. 2009;24(4):315-326.
11. Helito CP, Demange MK, Bonadio MB, et al. Anatomy and histology of the knee anterolateral ligament. *Orthop J Sports Med*. 2013;1(7): 2325967113513546.
12. Helito CP, Demange MK, Bonadio MB, et al. Radiographic landmarks for locating the femoral origin and tibial insertion of the knee anterolateral ligament. *Am J Sports Med*. 2014;42(10):2356-2362.
13. Hughston JC, Andrews JR, Cross MJ, Moschi A.Classification of knee ligament instabilities. Part I. The medial compartment and cruciate ligaments. *J Bone Joint Surg Am*. 1976;58(2):159-172.
14. Kang KT, Kim SH, Son J, Lee YH, Kim S, Chun HJ. Probabilistic evaluation of the material properties of the in vivo subject-specific articular surface using a computational model. *J Biomed Mater Res B Appl Biomater*. 2017;105(6):1390-1400.
15. Kang KT, Koh YG, Park KM, et al. The anterolateral ligament is a secondary stabilizer in the knee joint: a validated computational model of the biomechanical effects of a deficient anterior cruciate ligament and anterolateral ligament on knee joint kinematics. *Bone Joint Res*. 2019;8(11):509-517.
16. Kang KT, Koh YG, Son J, et al. Finite element analysis of the biomechanical effects of three posterolateral corner reconstruction techniques for the knee joint. *Arthroscopy*. 2017;33(8):1537-1550.
17. Kennedy MI, Claes S, Fuso FA, et al. The anterolateral ligament: an anatomic, radiographic, and biomechanical analysis. *Am J Sports Med*. 2015;43(7):1606-1615.
18. Kiapour A, Kiapour AM, Kaul V, et al. Finite element model of the knee for investigation of injury mechanisms: development and validation. *J Biomech Eng*. 2014;136(1):11002.
19. Kim YS, Kang KT, Son J, et al. Graft extrusion related to the position of allograft in lateral meniscal allograft transplantation: biomechanical comparison between parapatellar and transpatellar approaches using finite element analysis. *Arthroscopy*. 2015;31(12):2380-2391.
20. Klein Horsman MD, Koopman HF, van der Helm FC, Prose LP, Veeger HE. Morphological muscle and joint parameters for musculoskeletal modelling of the lower extremity. *Clin Biomech (Bristol, Avon)*. 2007; 22(2):239-247.
21. Kwon OR, Kang KT, Son J, et al. Biomechanical comparison of fixed- and mobile-bearing for unicomparmental knee arthroplasty using finite element analysis. *J Orthop Res*. 2014;32(2):338-345.
22. Lenhart RL, Kaiser J, Smith CR, Thelen DG. Prediction and validation of load-dependent behavior of the tibiofemoral and patellofemoral joints during movement. *Ann Biomed*. 2015;43(11):2675-2685.
23. Li G, Gil J, Kanamori A, Woo SL. A validated three-dimensional computational model of a human knee joint. *J Biomech Eng*. 1999;121(6): 657-662.
24. Lloyd DG, Besier TF. An EMG-driven musculoskeletal model to estimate muscle forces and knee joint moments in vivo. *J Biomech*. 2003; 36(6):765-776.
25. Marra MA, Vanheule V, Fluit R, et al. A subject-specific musculoskeletal modeling framework to predict in vivo mechanics of total knee arthroplasty. *J Biomech Eng*. 2015;137(2):20904.
26. Monaco E, Ferretti A, Labianca L, et al. Navigated knee kinematics after cutting of the ACL and its secondary restraint. *Knee Surg Sports Traumatol Arthrosc*. 2012;20(5):870-877.
27. Neyret P, Donell ST, Dejour H.Results of partial meniscectomy related to the state of the anterior cruciate ligament. Review at 20 to 35 years. *J Bone Joint Surg Br*. 1993;75(1):36-40.
28. Nitri M, Rasmussen MT, Williams BT, et al. An in vitro robotic assessment of the anterolateral ligament, part 2: anterolateral ligament reconstruction combined with anterior cruciate ligament reconstruction. *Am J Sports Med*. 2016;44(3):593-601.
29. Noyes FR, Mooar PA, Matthews DS, Butler DL. The symptomatic anterior cruciate-deficient knee. Part I: the long-term functional disability in athletically active individuals. *J Bone Joint Surg Am*. 1983; 65(2):154-162.
30. Parsons EM, Gee AO, Spiekerman C, Cavanagh PR. The biomechanical function of the anterolateral ligament of the knee. *Am J Sports Med*. 2015;43(3):669-674.
31. Pernin J, Verdonk P, Si Selmi TA, Massin P, Neyret P. Long-term follow-up of 24.5 years after intra-articular anterior cruciate ligament reconstruction with lateral extra-articular augmentation. *Am J Sports Med*. 2010;38(6):1094-1102.
32. Pomajzl R, Maerz T, Shams C, Guettler J, Bicos J. A review of the anterolateral ligament of the knee: current knowledge regarding its incidence, anatomy, biomechanics, and surgical dissection. *Arthroscopy*. 2015;31(3):583-591.
33. Ramaniraka NA, Terrier A, Theumann N, Siegrist O. Effects of the posterior cruciate ligament reconstruction on the biomechanics of the knee joint: a finite element analysis. *Clin Biomech (Bristol, Avon)*. 2005;20(4):434-442.
34. Rasmussen MT, Nitri M, Williams BT, et al. An in vitro robotic assessment of the anterolateral ligament, part 1: secondary role of the anterolateral ligament in the setting of an anterior cruciate ligament injury. *Am J Sports Med*. 2016;44(3):585-592.
35. Samuelson M, Draganich LF, Zhou X, Krumins P, Reider B. The effects of knee reconstruction on combined anterior cruciate ligament and anterolateral capsular deficiencies. *Am J Sports Med*. 1996;24(4): 492-497.
36. Schon JM, Moatshe G, Brady AW, et al. Anatomic anterolateral ligament reconstruction of the knee leads to overconstraint at any fixation angle. *Am J Sports Med*. 2016;44(10):2546-2556.
37. Shelburne KB, Torry MR, Pandy MG. Contributions of muscles, ligaments, and the ground-reaction force to tibiofemoral joint loading during normal gait. *J Orthop Res*. 2006;24(10):1983-1990.
38. Terry GC, Norwood LA, Hughston JC, Caldwell KM. How iliotibial tract injuries of the knee combine with acute anterior cruciate ligament tears to influence abnormal anterior tibial displacement. *Am J Sports Med*. 1993;21(1):55-60.
39. Trepczynski A, Kutzner I, Kornaropoulos E, et al. Patellofemoral joint contact forces during activities with high knee flexion. *J Orthop Res*. 2012;30(3):408-415.
40. Vincent JP, Magnussen RA, Gezmez F, et al. The anterolateral ligament of the human knee: an anatomic and histologic study. *Knee Surg Sports Traumatol Arthrosc*. 2012;20(1):147-152.
41. Wahl CJ, Westermann RW, Blaisdell GY, Cizik AM. An association of lateral knee sagittal anatomic factors with non-contact ACL injury: sex or geometry? *J Bone Joint Surg Am*. 2012;94(3):217-226.
42. Zens M, Niemeyer P, Ruhhammer J, et al. Length changes of the anterolateral ligament during passive knee motion: a human cadaveric study. *Am J Sports Med*. 2015;43(10):2545-2552.